

References

- [1] Mirzaei, M., Khaleghi, H., and Karimian, S. M., H., "An upwind algorithm for the solution of PNS equations", The Fifth Fluid Dynamics Conference, Iranian Society of Physics, Ferdosi University, Iran, August 25-27, 1998.
- [2] Vigneron, Y., C., Rakich, J., V., and Tannehill, J., C., "Calculation of Supersonic Viscous Flow over Delta Wings with Sharp Supersonic Leading Edges", AIAA Paper 78-1137, July 1978.
- [3] Lawrance, S. Tannehill, J., C., and Chaussee, C., S., "An Upwind Algorithm for the Parabolized Navier-Stokes Equations", AIAA paper 86-1117, 1986.
- [4] Thompson, D., S., and Matus, R., J., "Conservation Errors and Convergence Characteristics of Iterative Space Marching Algorithm", AIAA Journal, Vol. 29, No.2, Feb. 1991, pp. 227-234.
- [5] Ota, D., K., Chakravathy, S., R., and Darling, J. C., "An Equilibrium Air Navier-Stokes Code for Hypersonic Flows", AIAA paper 88-0419, 1988.
- [6] Thompson, D., S., and Anderson, D., A., "A Pseudo-Unsteady Approach for Predicting Steady Supersonic Flows", AIAA Paper 87-0541, 1987.
- [7] Lombard C. K., Venkatapathy E., and Bardina, J., "Universal Single Level Implicit Algorithm for Gas Dynamics" AIAA Paper 84 - 1533, 1984.
- [8] Rubin, S. G., and Reddy, D. R., "Analysis of Global Pressure Relaxation For Flows with Strong Interaction and Separation", Computer and Fluids, Vol. 11, No. 15, 1987, pp. 361-377.
- [9] Rakich, J. V., "Iterative PNS Method for Attached Flows with Upstream Influence" AIAA Paper 83-1955, 1983.
- [10] Power, G. D., "A Novel Approach for Analyzing Supersonic High Reynolds Number Flow Separation", AIAA Paper 90-0764, 1990.
- [11] Barnet M., and Davis, R. T., "Calculation of Supersonic Flows with Strong Viscous - Inviscid interaction" AIAA Journal, Vol. 24, No. 12, DEc. 1986, pp. 1949-1955.
- [12] Miller, J. H., and Tannehill, J. D., "Computation of Supersonic Flow with Embedded Separated Region Using an Efficient PNS Algorithm, AIAA-97, 1942.
- [13] Rehyner, T. A., and Flugge-Lotz, "The Interaction of a Shock Wave with a Laminar Boundary Layer", International Journal of Non-Linear Mechanics, vol. 3, 1968, pp. 173-199.
- [14] White, F., "Viscous Fluid Flow", McGrawhill Inc., New York, 1991.
- [15] Caret, J., E., "Numerical Solutions of the Navier-Stokes Equations for the Supersonic Flow over a Two Dimension Compression Corner", NASA TR R-385, July, 1972.
- [16] Hung. C., M., and Mac Cormack, R., W., "Numerical Solutions of Supersonic and Hypersonic Laminar Compression Corner Flows", AIAA Journal, Vol, 14, No. 4, April 1979. pp. 475-481.
- [17] Thomas, J., L. and Walters, R., W., "Upwind Relaxation Algorithms for the Navier-Stokes Equations", AIAA Journal, Vol. 25, No.4, April 1987, pp. 527-534.

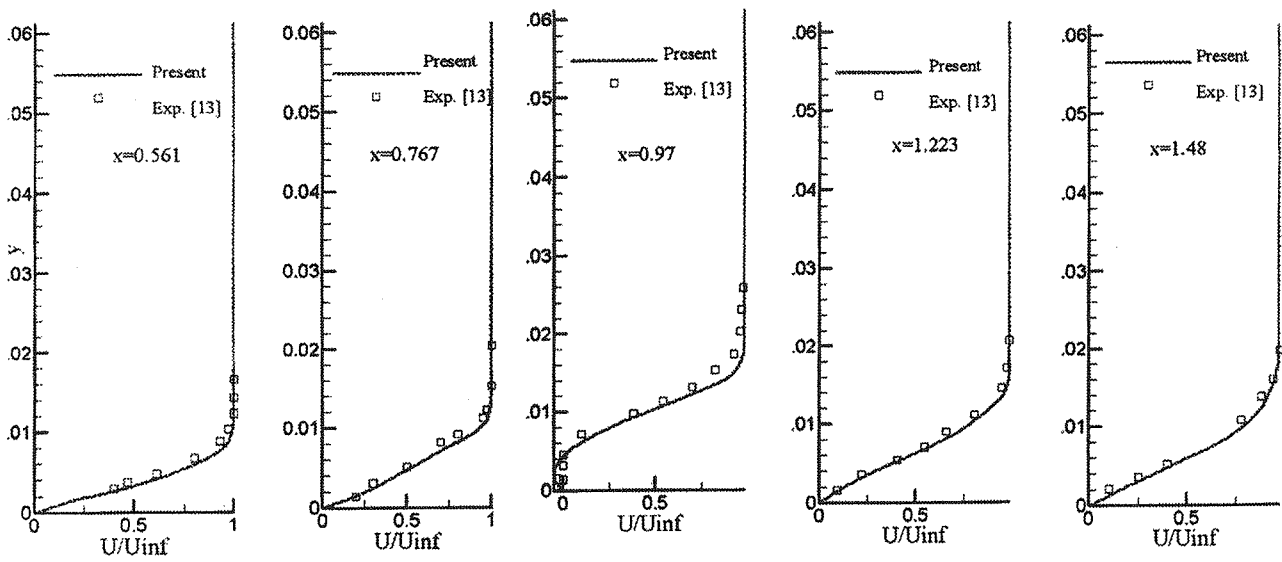


Fig. (15) Velocity profiles for shock impingement

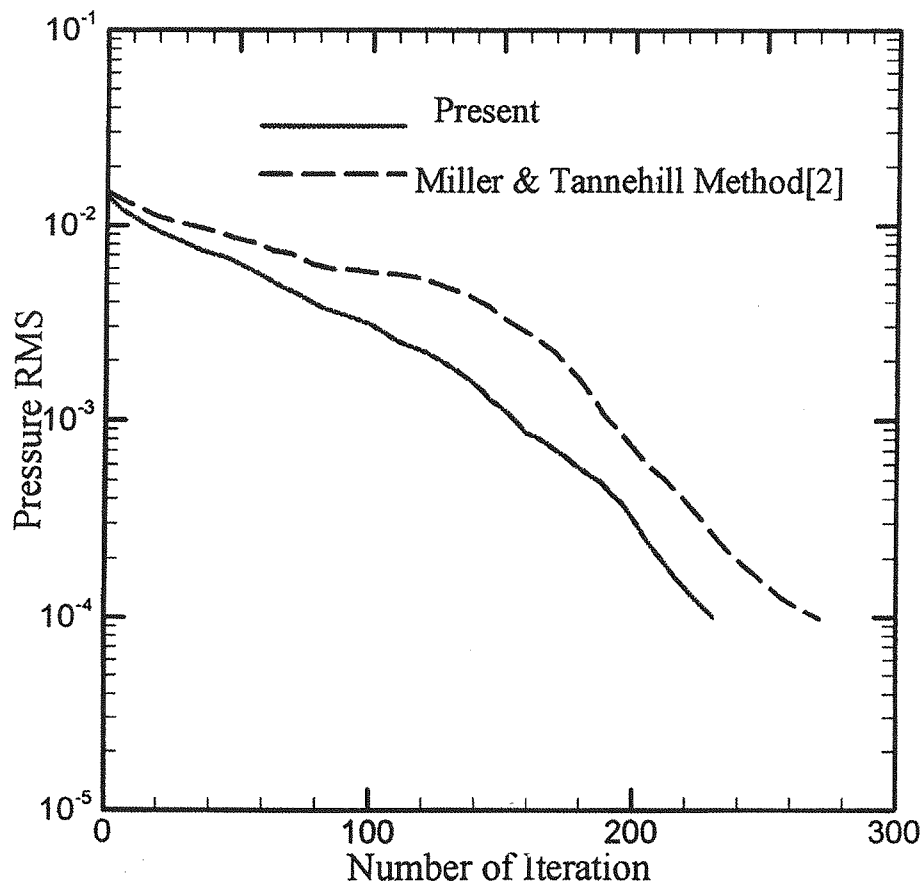


Fig. (16) Convergence trend for shock impingement

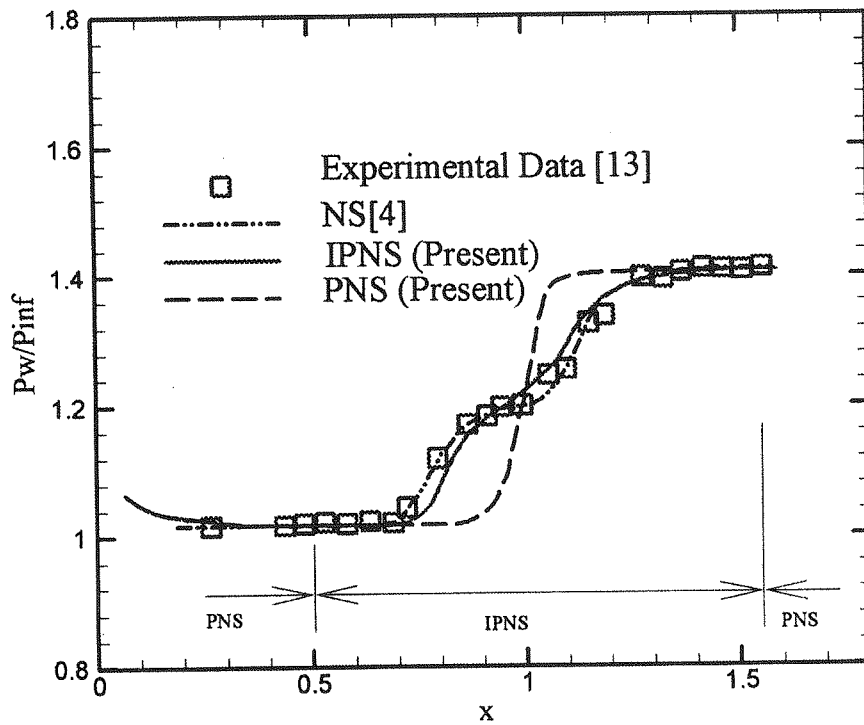


Fig. (13) Wall pressure results for shock impingement

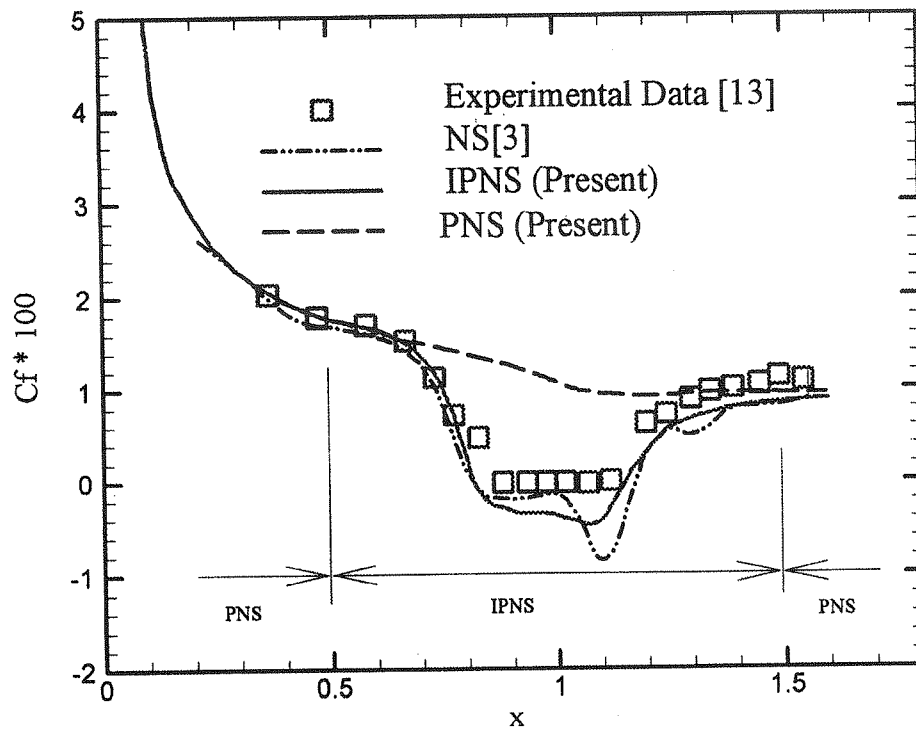


Fig. (14) Friction factor results for shock impingement

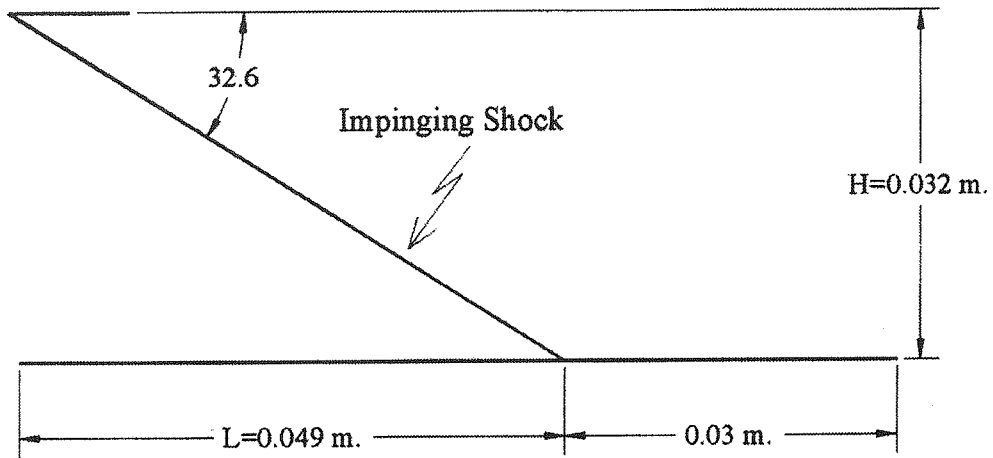


Fig. (11) Geometry of shock impingement

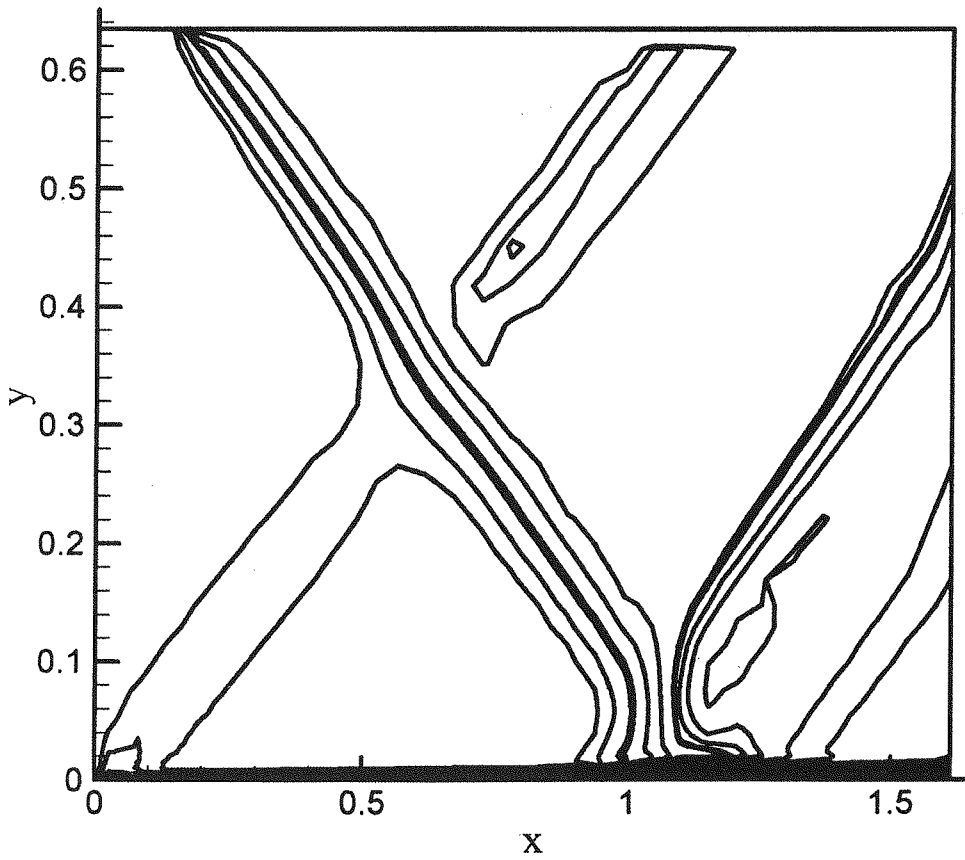


Fig. (12) Mach number contour for shock impingement

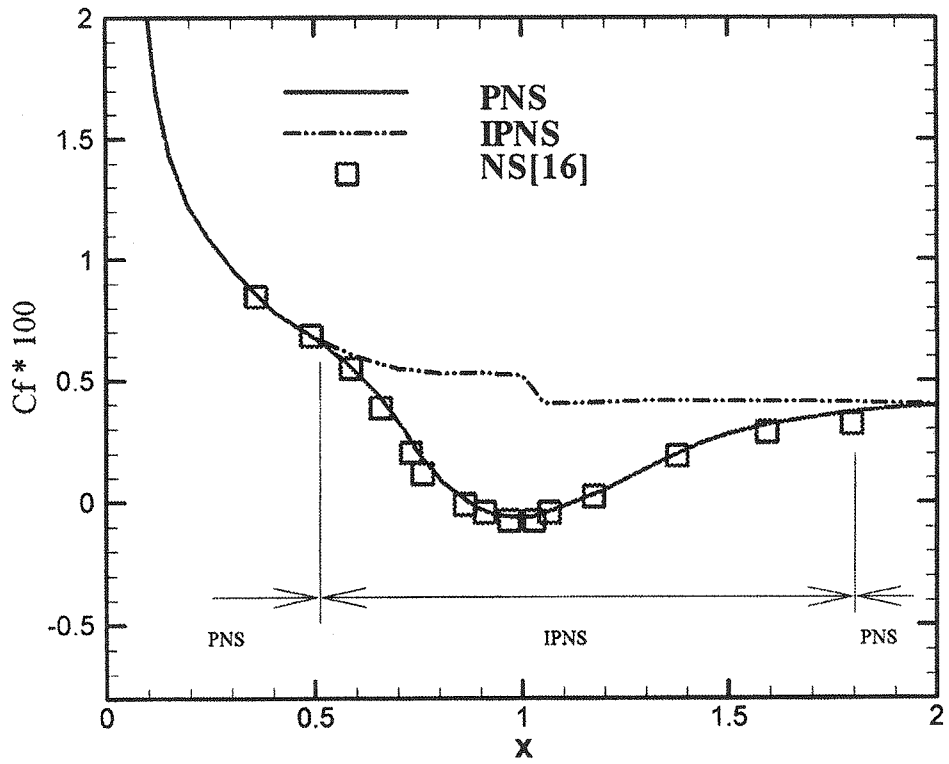


Fig. (9) Friction factor results for a 10 degrees ramp

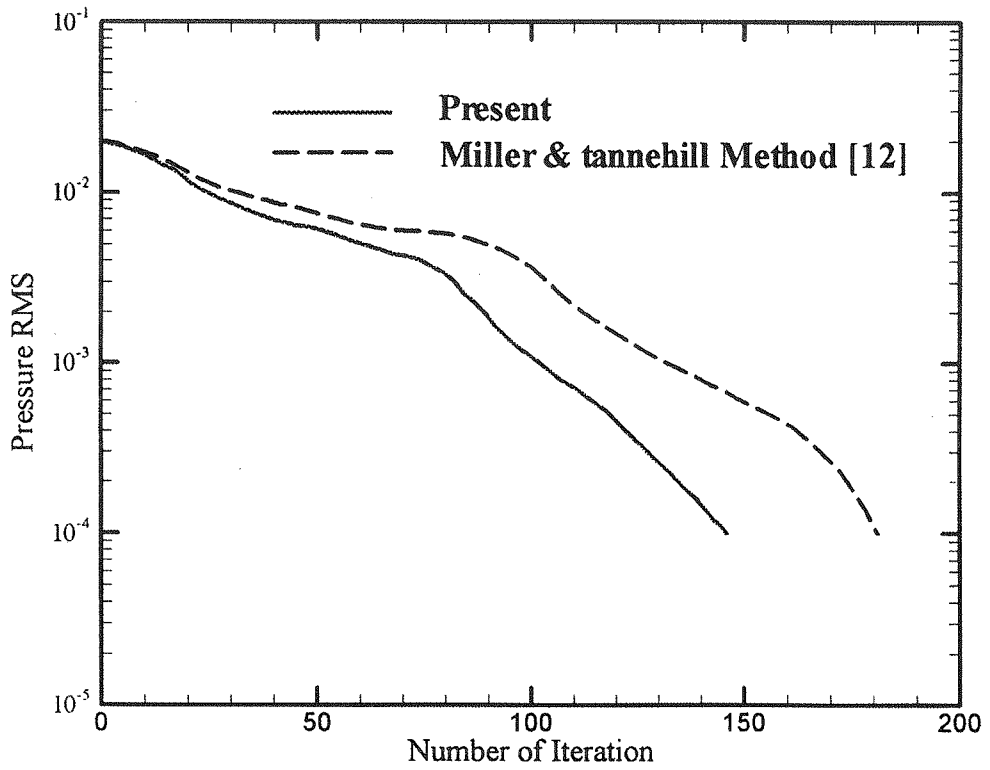


Fig. (10) Convergence trend for a 10 degrees ramp

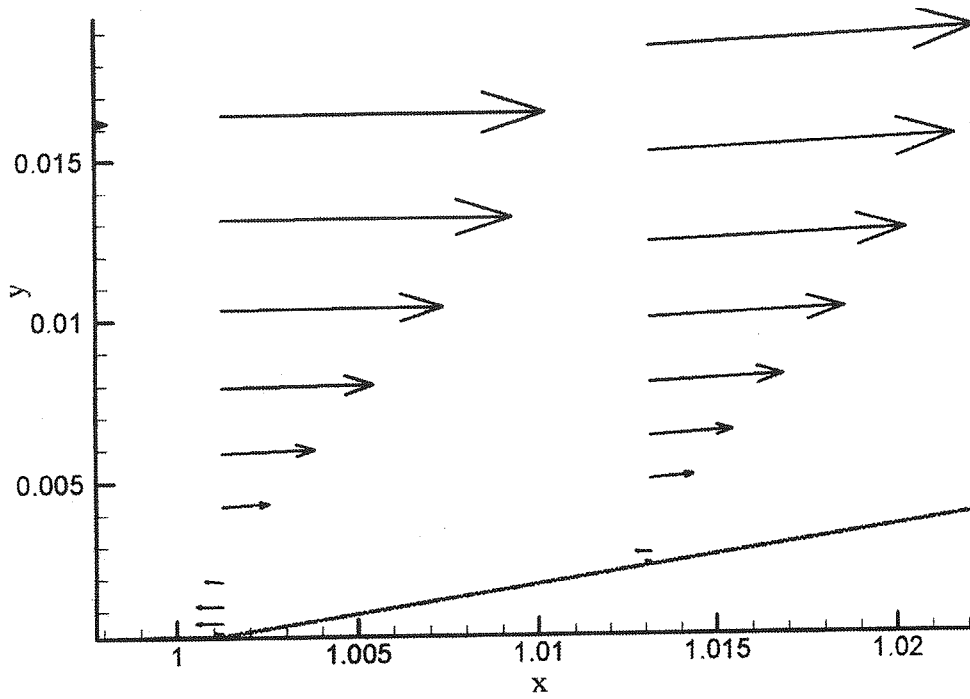


Fig. (7) Velocity distribution in IPNS region for a 10 degrees ramp

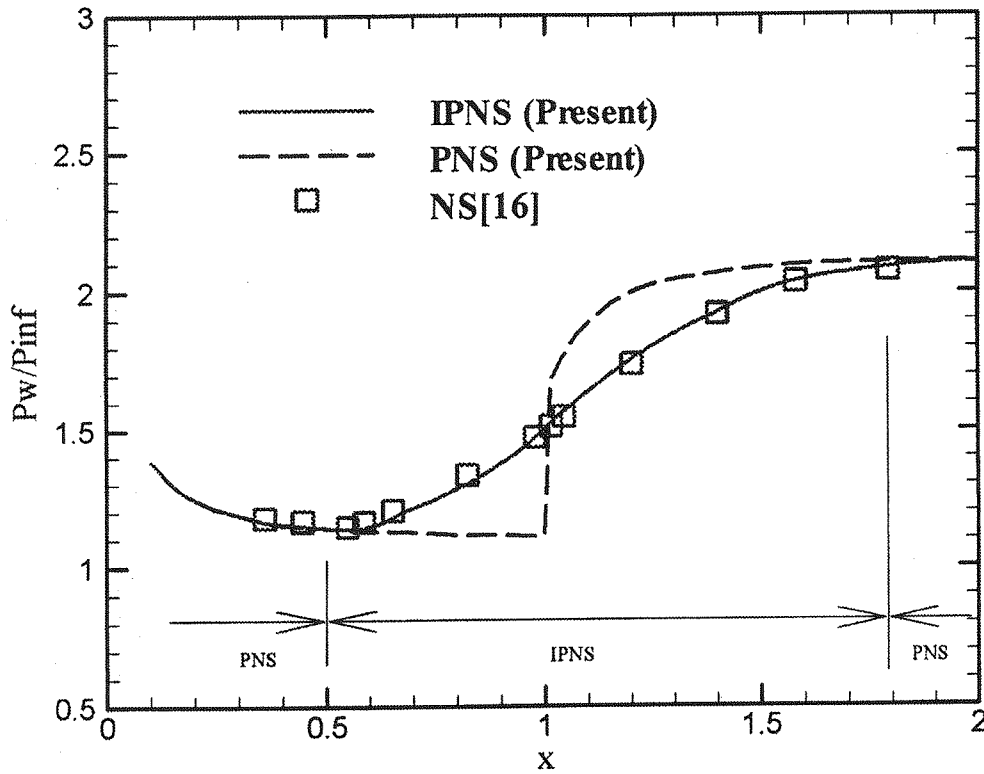


Fig. (8) Wall pressure results for a 10 degrees ramp

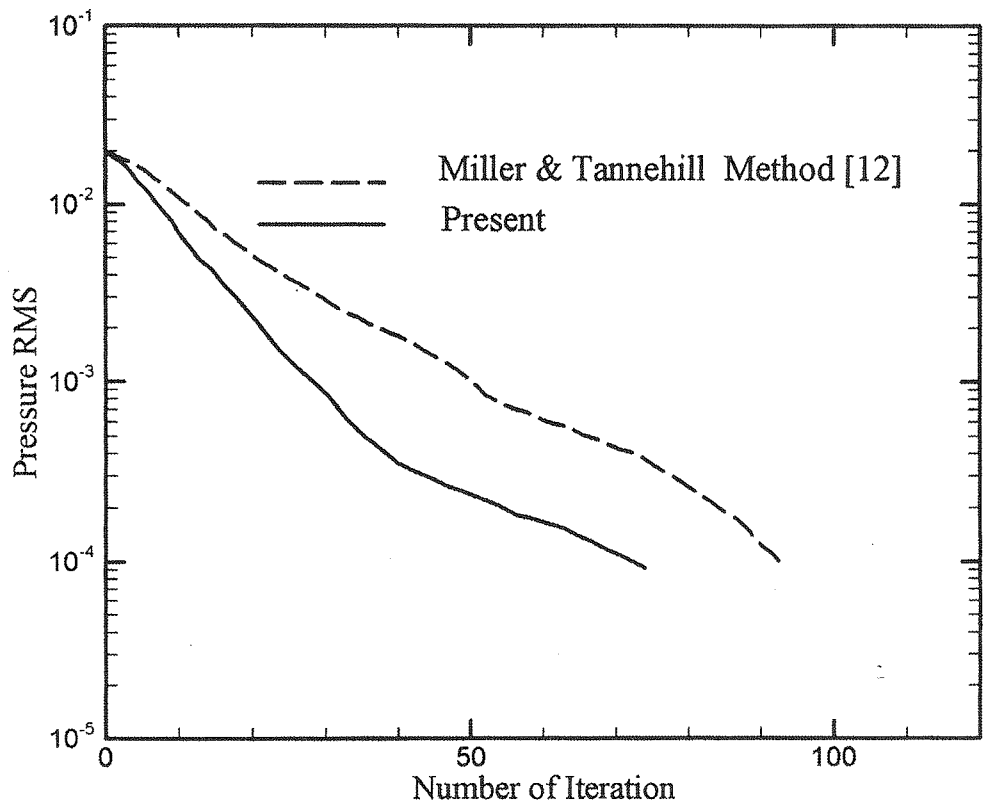


Fig. (5) Convergence trend for a 5 degrees ramp

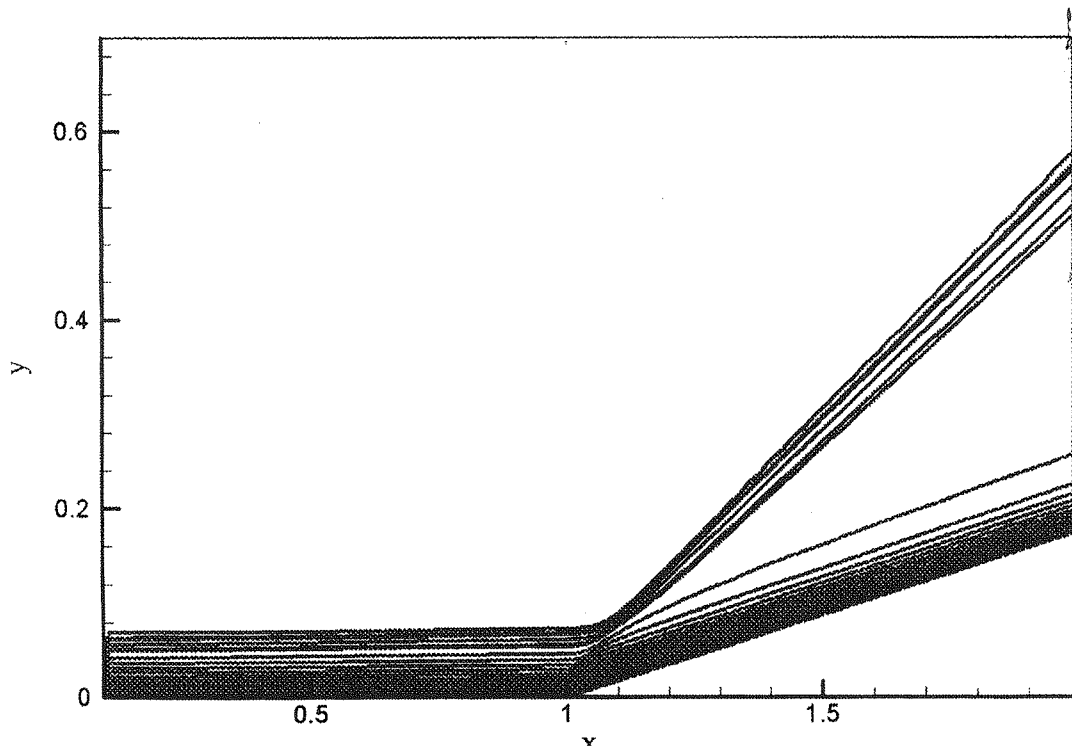


Fig. (6) Mach number contours for a 10 degrees ramp

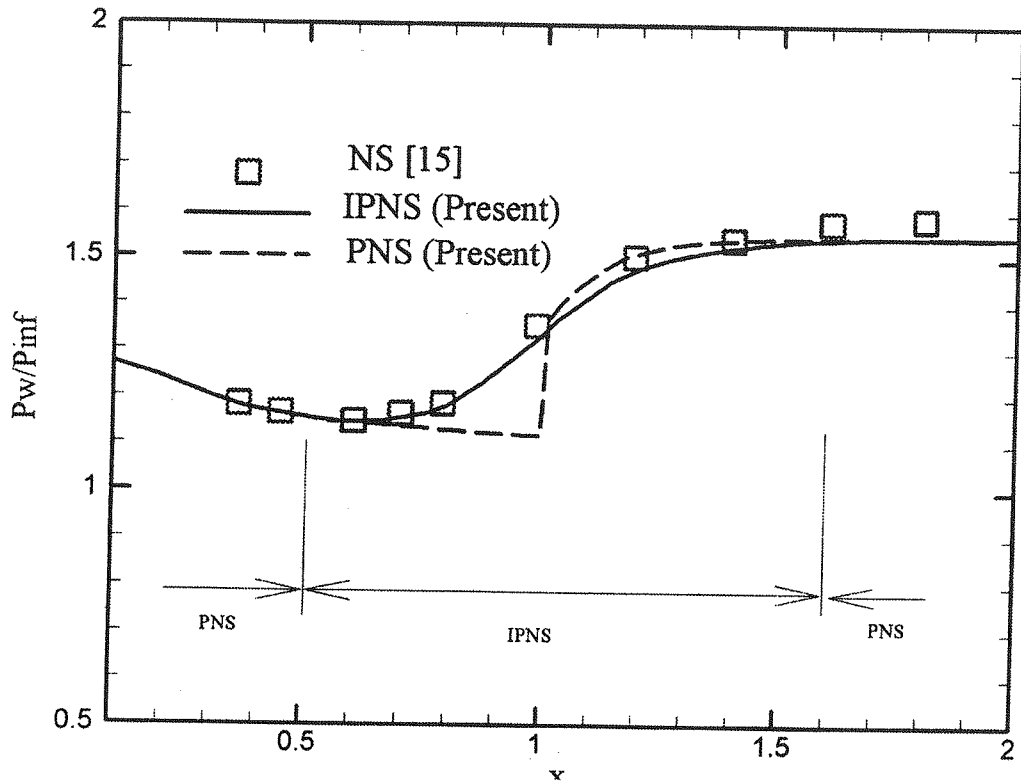


Fig. (3) Wall pressure results for a 5 degrees ramp

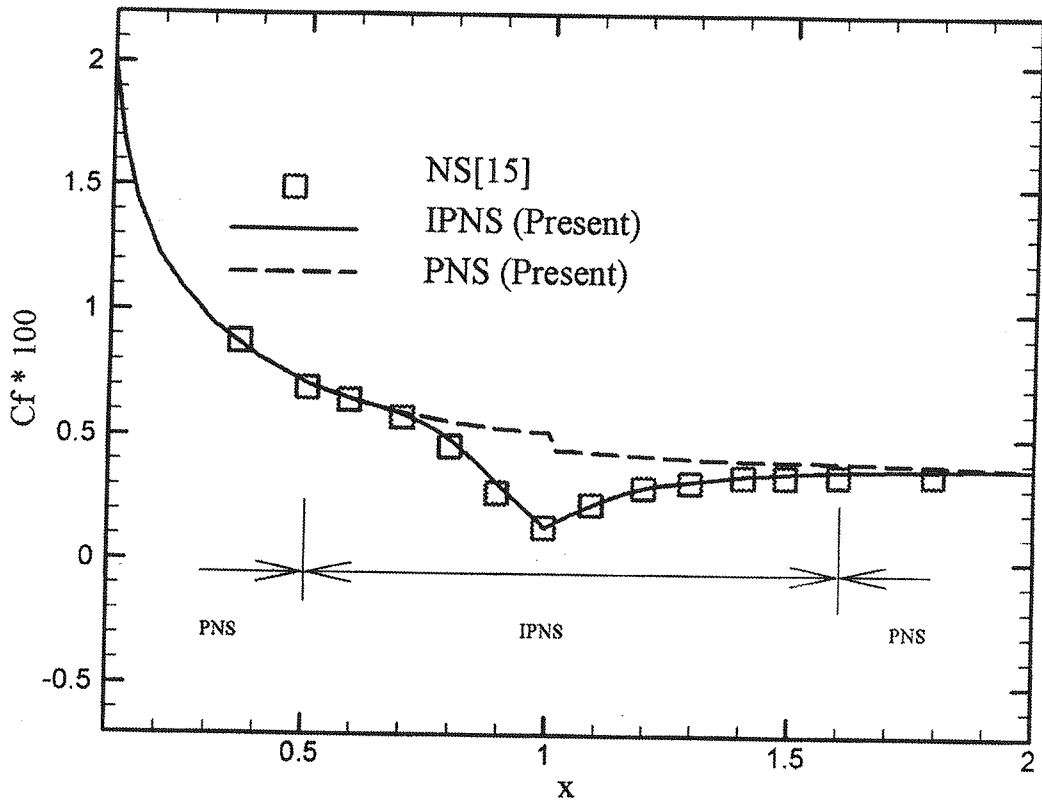


Fig. (4) Friction factor for a 5 degrees ramp

cluding regions with strong upstream effects. The developed algorithm has been applied to several test cases. The results are in good agreement with NS computation and experimental data. Performance of the present method has been compared with the performance of the method used in Ref. 12. It has been shown that the present method converges faster, and this reduces the CPU time some thing between 10% to 18%. Eventhough the presented test cases were limited to simple geometries, but it is hoped

that development of this method for computation of flows around complex vehicles will also reduce the CPU time.

9 - Acknowledgments

Authors would like to express their sincere thanks to Shahid Bakeri Industrial and Research Group for their support during the course of the work. Special thanks goes to Mr. Bromandy for his continuous encouragement during this study.

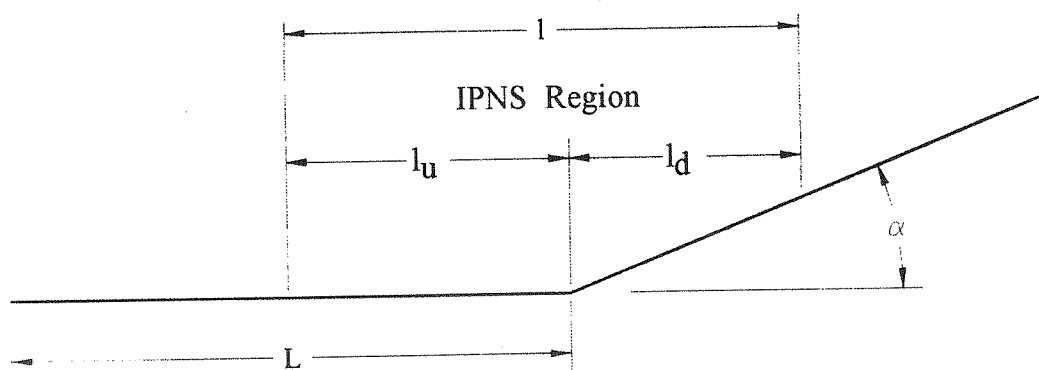


Fig. (1) Length definitions for detection of IPNS region

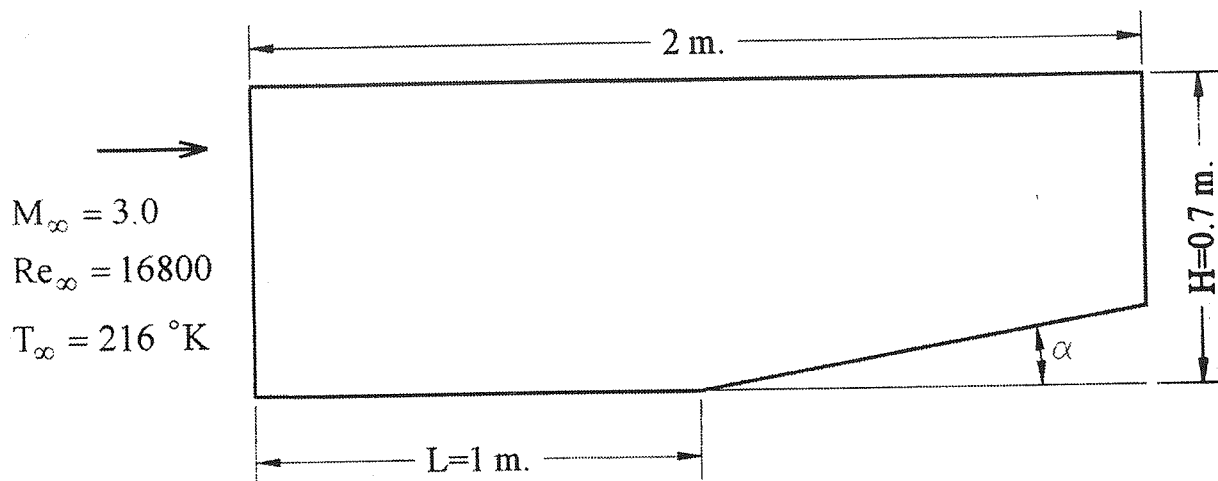


Fig. (2) Geometry and conditions of flow over a ramp

where the summation is over all points in the IPNS region, ($k=1, 2, \dots K_{max}$).

The second case is a supersonic flow over a 10° ramp. All the conditions in this case are the same as those of previous one. The finest grid used for this problem contains 110 points in normal direction and 320 points in streamwise direction with 219 point in the IPNS region, i.e. $0.5 < x < 1.8$. Figures 6 and 7 show Mach number contours and velocity vectors, respectively. Distribution of pressure and friction factor along the wall are shown in Figs. 8 and 9, respectively. In these figures the IPNS results are compared with the NS results of Hung and Mac Cormack [16]. As seen the agreement between these results are excellent. In Fig. 10 convergence trend of pressure RMS obtained from the present method and the method of Ref. 12 are compared with each other. In the present method the number of iterations required for convergence up to 10^{-4} is about 82% of those reported from Ref. 12.

The third case includes impingement of an oblique shock on a laminar boundary layer developed on a flat plate, as shown in Fig. 11. The shock angle θ is 32.6° , the wall is considered adiabatic, and the free stream conditions are

$$M_\infty = 2.0 \quad Re_L = 2.96 \times 10^5 \quad T_\infty = 165^\circ \text{ K}$$

The characteristic length is set equal to the x-position of impinging point, i.e. $L=0.049$ m. Marching is started from the edge of the plate with very small step size and is continued until position $x=0.041$. Then a constant step size is used until station $x = 1.61$, which is the end of solution domain. As seen in Fig. 10, the height of solution do-

main is set equal to 0.65. Conditions behind the oblique shock along the top boundary is determined based on Rankine-Hugoniot conditions. There are 170 grid points located in the normal direction and 420 nodes in the streamwise direction. From the latter one 272 grid points are located in the IPNS region, i.e. $0.5 < x < 1.53$. Mach number contours are shown in Fig. 12 and distributions of pressure and friction factor along the wall are shown in Figs. 13 and 14, respectively. In these figures IPNS results, and the conventional PNS results NS results of Thomas and Walter [17] are compared with experimental data presented by Hakkinan et. al. [13]. It should be noted that in this case a significant region of separation exists in IPNS region. It is noted that the approximation used for the stability of the method in separated regions does affect the detail of the separation as shown in Figs. 13 and 14. However, for such a difficult test case, the IPNS results follow the experimental data very well, and also the extent of the separation region is in excellent agreement with the NS results and experimental data. In Fig. 15 velocity profiles of IPNS in five stations, are compared with the experimental data. As seen the agreement is very well. Convergence trend of pressure RMS obtained from the present method and that of the method used in Ref. 12 are shown in Fig. 16. It can be seen that with the present number of iterations required for convergence of 10^{-4} , decreases about 14%.

8- Conclusions

In this paper a method is presented for the calculation of pressure gradient in the streamwise direction to develop a PNS solver for computation of flow fields in-

relations since approximations have been used in derivation of the above correlation functions. With $\sigma_{1,2} \approx 1.2$ good agreement is observed between the numerical results and experimental data. For more details about these functions see Ref. 12. Using relation (6), l_v/δ_L is obtained as:

$$\frac{l_u}{L} = F_{1,2} \frac{\sqrt{C_w}}{\sqrt{Re_L}} \left(5.0 + \left(0.2 + 0.9 \frac{T_w}{T_{aw}} \right) (\gamma - 1) M_\infty^2 \right) \quad (10)$$

in which F_1 and F_2 can be substituted from either Eq. (8-a) or Eq. (9-a). Note that the right-hand side of Eq. (10) is only a function of free stream conditions and solution domain geometry. This equation together with Eq. (8-b) or (9-b) can be easily used for detection of IPNS regions in flow fields over compression ramps and shock impingement on a flat plate. As stated previously it is the above correlations that are used in the present paper.

6 - Results

The proposed IPNS algorithm is tested for three cases of two dimensional laminar flow including regions with strong upstream effects. The first test case is a supersonic flow over a 5° ramp. Wall temperature is 606° K and L is considered as 1m. The free stream conditions are:

$$M_\infty = 3.0 \quad Re_L = 1.68 \times 10^4 \quad T_\infty = 216^\circ \text{ K}$$

This problem has been solved in Ref. 15 using Navier-stokes solver. Although the flow is not separated, the ramp induces significant upstream effects. From the free stream conditions at the edge of the plate, solution is marched with a very small step size until $x=0$. It must be noted that all of

the lengths, discussed in this section, are non-dimensionalized with characteristic length of L . The computation then resumed using a larger constant step size toward the end of the domain. The height and length of the computational domain are 0.7 and 2.0 respectively. The finest grid used to show grid independent results, includes 100 points in the normal direction and 270 points in the streamwise direction (from $x = 0.1$ to $x = 2$). There are 156 points located in the IPNS region, i.e. $0.5 < x < 1.6$. Distributions of pressure and friction factor along the surface are compared with the solution of NS computation [5] in Figs. 3 and 4, respectively. The excellent agreement between the IPNS and NS results proves the accuracy of our calculation in IPNS region. Distribution of friction factor which is defined as

$$C_f = \frac{\mu}{(1/2) \rho_\infty U_\infty^2} \left(\frac{\partial u}{\partial n} \right)_{\text{wall}} \quad (11)$$

compares very good in the whole domain; see Fig. 4. The pressure distribution however is a bit under-predicted from $x=1.2$ to the end of the domain. As seen there is a larger difference between results of PNS and IPNS, specially after the beginning of IPNS region. In Eq. (11) "n" denotes the normal direction to the wall. Convergence trend based on the root mean square (RMS) of the relative change in pressure, in the IPNS region, is shown in Fig. 5. As seen in this figure, number of iterations required for convergence is nearly 20% less than the one used in Ref. 12. The root mean square is defined as:

$$RMS = \sqrt{\frac{1}{K \max} \sum_{k=1}^{K \max} \left(\frac{P_k^{n+1} - P_k^n}{P_k^n} \right)^2} \quad (12)$$

required CPU time and convergence rate would be decision-making for choosing of the method for evaluating pressure gradient term.

5 - Determination of IPNS Application Region

In this paper the IPNS region is detected automatically. Simple flow fields with single IPNS region is considered here. The IPNS region is determined using a correlation function which is derived based on the geometry of solution domain and flowfield parameters. For instance, Fig. 1 shows the range of IPNS region for supersonic flow over a ramp. As indicated, the IPNS region is divided into two parts, a first part with length of l_u , called upstream length, and a second part with length of l_d called downstream length. Correlation functions determine the ratio of l_u / δ_L , where δ_L is the boundary layer thickness at L . The experimental relation given by White [14] is used to specify the value of δ_L , as:

$$\delta_L = \frac{L \sqrt{C_w}}{\sqrt{Re_L}} \left[50 + \left(0.2 + 0.9 \frac{T_w}{T_{aw}} \right) (\gamma - 1) M_\infty^2 \right] \quad (6)$$

where in this relation:

$$C_w = \rho_w \mu_w / \rho_\infty \mu_\infty \cong (T_w / T_\infty)^{-1/3}$$

and

$$T_{aw} = T_\infty \left(1 + \frac{\gamma - 1}{2} \sqrt{Pr} M_\infty^2 \right)$$

in which $Pr=0.72$

Based on dimensional analysis, l_u/δ_L is assumed as a function of four dimensionless quantities of free stream Mach number (M_∞), Reynolds number (Re_L), ratio of wall

temperature to adiabatic wall temperature (T_w/T_{aw}), and relative pressure change in inviscid flow ($\Delta p/p_\infty$). For a case with adiabatic wall, correlation function of l_u/δ_L becomes:

$$\frac{l_u}{\delta_L} = F \left[(\Delta P/P_\infty)^a, (M_\infty)^b, (Re_L)^c \right] \quad (7)$$

The constant a , b and c have been specified in Ref. 12 for flow fields of 2-D compression ramp and shock impingement on a flat plate. In this reference IPNS algorithm, itself, is used for determining these constants. By applying IPNS algorithm for different values of $\Delta P/P_\infty$, M_∞ and Re_L in the whole solution domain, a variety of numerical data is produced. Now for each problem, constants of the correlation function are determined using least square statistical analysis. Beginning of the IPNS region is indicated whenever the friction coefficient deviates 1% from its value on a flat plate, and the end of this region is determined whenever this coefficient becomes constant. The following correlations have been derived by applying the above method [12]. For flow over compression ramps (see Fig. 2) we have:

$$F_1 = \frac{l_u}{\delta_L} = \sigma_1 \left(\frac{\Delta P}{P_\infty} \right)^{3/8} \frac{Re_L^{3/8}}{M_\infty^{3/2}} \quad (8-a)$$

$$\frac{l_u}{l_d} = 2.6 \quad (8-b)$$

and for shock impingement flow fields (see Fig. 11) we have:

$$F_2 = \frac{l_u}{\delta_L} = \sigma_2 \left(\frac{\Delta P}{P_\infty} \right)^{1/5} \frac{Re_L^{2/5}}{M_\infty} \quad (9-a)$$

$$\frac{l_u}{l_d} = 2.3 \quad (9-b)$$

Coefficients σ_1 and σ_2 appear in these cor-

$$\left(\frac{\partial p_i^{n+1}}{\partial \xi_{i+1}^{n+1}}\right) = \left[\omega - (1-\omega)\left(\frac{1}{S} + 1\right)\right] \frac{p_{i+1}^{n+1} - p_i^{n+1}}{\Delta \xi} + (1-\omega) \left[\frac{p_{i+2}^{n+1} + \frac{1}{S} p_{i+1}^{n+1} - \frac{1}{S} + 1}{\Delta \xi}\right] p_i^{n+1} \quad (5)$$

where $S = \Delta t / \Delta \xi$. In regions where IPNS algorithm is applied, implementation of relation (5) requires the information on downstream boundary of such regions (due to presence of p_{i+2}^n). In Ref. 11, Neumann boundary condition is applied for pressure. The pressure gradient is specified using supersonic small disturbance theory and considering self similar nature of boundary layer. The approach of Ref. 8 is to fix the pressure gradient using its value calculated from conventional PNS solver. What we have applied in this paper is to equate the pressure gradient with its value at the previous marching step. This condition is based on the assumption that pressure is being linearly varied close to the downstream boundary of these regions. The advantage of this approach is that it can be easily extended to a 3-D IPNS code. It must be noted that an appropriate value of S falls between 0.95 and 1.03. In this range the number of iterations are minimized. The value less than 0.75 causes solution instability. Results obtained in this paper are all with $S=1.0$

3 - Modification Required in Separated Regions

As stated previously, space marching method would be stable if the velocity component in the streamwise direction is always positive. In separated regions however, this will not happen. But since the mainstream flow is supersonic the negative velocities in separated regions are small, and thus one way is to simply eliminate all

the convection terms with negative streamwise velocities [12]. Instead of eliminating these terms, the other approach adopted by Ref. 13 is to keep their absolute values. In Ref. 11, only a fraction of these absolute values is employed. Refs 6 and 10 have compared results of the above approaches and demonstrated that all of them result in the same solution; this fact is also observed in the present paper.

In separated regions, the governing equations are completely elliptic, therefore ω should be zero. In the present work, it is shown that the convergence rate would be optimum if $\omega=0$ between surface and boundary layer edge in the separated regions. This, in fact is equal to solving boundary layer equations in each marching step with a prescribed pressure distribution. The value of ω is determined using the simple criteria of:

$$\omega = \begin{cases} 1 & u < u_s \\ 0 & u > u_s \end{cases}$$

where u_s is the nondimensional value of velocity which is set equal to 0.99.

4- Solution Algorithm of PNS Equations

In the present work finite volume method is used for the solution of two dimensional/axisymmetric PNS equations in the curvilinear coordinate. The components of flux vector are evaluated using second-order upwind method of Roe; for more details see Ref. 1. This algorithm has been previously used in Ref. 12. The main difference between the developed PNS algorithm IPNS in the present work, and that of Ref. 12 is the method of evaluating pressure gradient terms. A comparison between the

where σ is a safety factor ranging from 0.75 to 0.95, and M_ξ is Mach number of flow in the ξ direction. Using Vigneron's method Eq. (2) becomes:

$$\frac{\partial \bar{E}_i^*}{\partial \xi} + \frac{\partial \bar{F}_i}{\partial \eta} + \frac{\partial \bar{E}_p}{\partial \xi} + \alpha \bar{H}_i = \frac{\partial \bar{F}_v^*}{\partial \eta} + \alpha \bar{H}_v^* \quad (3)$$

in which

$$\bar{E}_i = \bar{E}_p + \bar{E}_i^*$$

and

$$\bar{E}_p = \frac{1}{J} [\xi_x E_p + \xi_y F_p]$$

$$\bar{E}_i^* = \frac{1}{J} [\xi_x E_i^* + \xi_y F_i^*]$$

$$F_p = \begin{bmatrix} 0 \\ 0 \\ (1-\omega)p \\ 0 \end{bmatrix} \quad E_p = \begin{bmatrix} 0 \\ (1-\omega)p \\ 0 \\ 0 \end{bmatrix}$$

$$F_i^* = \begin{bmatrix} \rho v \\ \rho uv \\ \rho v^2 + \omega p \\ (E_i + p)v \end{bmatrix} \quad E_i^* = \begin{bmatrix} \rho u \\ \rho u^2 + \omega \\ \rho uv \\ (E_i + p)v \end{bmatrix}$$

In conventional PNS solvers, the $(1-\omega)$ fraction of pressure gradient is either eliminated, or evaluated using backward differencing. Several investigators have modified the conventional PNS solvers to permit the calculation of flows with strong upstream effects. One of the first attempts in modification of conventional PNS solvers is the work of Rakich [9]. His approach was to use Vigneron's method in which the $(1-\omega)$ fraction of pressure gradient is calculated using forward differencing in the regions with strong upstream effects; similar approaches have been also applied in Refs. 10 and 11. Thomson and Anderson [6] utilized

a second order expression for the pressure gradient, which includes a dissipation term to improve the stability of the method.

The PNS equations with a modified pressure term is applied either to separated regions or the whole domain. The basic approach in all of the references is to iteratively solve these equations in a selected domain. The procedure is that the solution is marched from the beginning of the domain toward the end of it. Such a procedure is iterated until a converged solution is obtained. This PNS algorithm called developed algorithm, is also named as Iterative Parabolized Navier-Stokes (IPNS) algorithm. If the IPNS code is only applied to regions with strong upstream effects (e.g. separated regions), these regions should be either predicted initially or detected automatically. In Ref. 12, for instance, a method has been proposed for automatic detection of these regions. The method of Ref. 12 is adopted in the present paper and will be discussed in section 5.

In IPNS algorithm of the present paper, correction of the pressure gradient is performed using Vigneron's approach with an additional pseudo-time derivative of pressure multiplied by $(1-\omega)$. Therefore the pressure gradient term becomes:

$$\left(\frac{\partial p}{\partial \xi} \right)_{i+1}^{n+1} = \omega \frac{p_{i+1}^{n+1} - p_i^{n+1}}{\Delta \xi} + (1-\omega) \left[\frac{p_{i+2}^n - p_i^{n+1}}{\Delta \xi} - \frac{p_{i+1}^{n+1} - p_i^{n+1}}{\Delta t} \right] \quad (4)$$

in which superscript "n+1" indicates the present iteration level, and subscript "i+1" denotes the current marching step being computed. After rearranging relation (4) we get:

caus of the difficulties due to the matching of two codes, it is preferred to apply a NS code for the whole domain, although it would be slower. The other approach adopted by researchers [4-7], is to solve NS equations in supersonic region using space marching technique. Since NS equations should be solved iteratively in each marching step, this method becomes very slow. The last approach is to develop a technique by which a PNS code can be used for the solution of flows with embedded separated regions. The modified PNS code may be used either for the whole solution domain [8], or only in the regions with strong upstream effects [9, 10]. The latter choice needs less computational efforts, and this makes the calculation faster. In this paper we have adopted such an approach.

Detection of regions with strong upstream effects is automatically done by the code. Although development of PNS codes for the calculation of separated regions are basically similar to each other, the main difference is their approach for the calculation of pressure gradient term in the streamwise direction. In the present paper, the pressure gradient term is calculated using a new method which considerably reduces computational efforts.

2 - Governing Equations

Based on the physical assumptions applied to the NS equations, different types of PNS equations have been derived. The main assumptions are, 1) elimination of transient terms, 2) elimination of viscous derivatives in the streamwise direction and 3) modification of pressure gradient term in the streamwise direction for stability considerations. The steady state two dimen-

sional/axisymmetric ($\alpha = 0, 1$) NS equations in the computational domain (ζ, η) is given by:

$$\frac{\partial \bar{Q}}{\partial \tau} + \frac{\partial \bar{E}}{\partial \xi} + \frac{\partial \bar{F}}{\partial \eta} + \alpha \bar{H} = 0 \quad (1)$$

in which:

$$\bar{E} = \bar{E}_i - \bar{E}_v \quad \bar{F} = \bar{F}_i - \bar{F}_v \quad \bar{H} = \bar{H}_i - \bar{H}_v$$

Applying assumptions 1 and 2, Eq. (1) becomes:

$$\frac{\partial \bar{E}_i}{\partial \xi} + \frac{\partial \bar{F}_i}{\partial \eta} + \alpha \bar{H}_i = \frac{\partial \bar{F}_v^*}{\partial \eta} + \alpha \bar{H}_v^* \quad (2)$$

in which the superscript * indicates that the corresponding terms do not include viscous derivatives in marching direction ξ . PNS equations are hyperbolic-parabolic in the streamwise direction. Eigenvalue analysis of these equations dictates that a space marching method is stable if 1) flow is supersonic in the inviscid part of it, 2) velocity component in the streamwise direction is positive in the subsonic region, and 3) pressure gradient in the streamwise direction is corrected to eliminate the elliptical behavior of the equations in subsonic region. Vigneron's method [2] is the most common approach for the correction of pressure gradient term. Vigneron showed that the nature of PNS equations remains hyperbolic-parabolic in the subsonic regions without separation, if only a fraction of pressure gradient in the streamwise direction is included. Using eigenvalue analysis the amount of this fraction, called ω , is obtained as:

$$\omega = \min \left[\frac{\sigma \gamma M_\xi^2}{1 + (\gamma - 1) M_\xi^2}, 1 \right]$$

A New Approach for the Solution of Supersonic Flows with Embedded Separated Regions Using PNS Equations

M. Mirzaei
Ph.D. Candidate
Mechanical Engineering Department ,
Tarbiat Modarres University

H. Khaleghi
Assistant Professor
Mechanical Engineering Department ,
Tarbiat Modarres University

S.M. H. Karimian
Assistant Professor
Aerospace Engineering Department ,
Amirkabir University of Technology

Abstract

Conventional PNS codes cannot be used for the solution of supersonic flows with separated regions. In this paper a new method is presented for the modification of a conventional PNS code to solve supersonic flows with embedded separated regions or regions with strong upstream effects. Flux vector components are calculated using Roe's second order scheme. In the above-mentioned regions, which are detected automatically by the code, PNS equations are solved. The addition of a pseudo-time derivative of pressure has highly increased the efficiency of the code. Two dimensional calculations of supersonic flow over compression ramps and oblique shock impingement on a flat plate are made to validate the new method. Comparison of the results with experimental data, and results of Navier-Stokes computations demonstrates the accuracy and excellent performance of the present method.

Key words

PNS, Embedded Regions, Upwind, Roe's Method

Introduction

PNS equations have been extensively used for the numerical simulation of steady supersonic viscous flows [1-3]. Space marching in the streamwise direction is the basic approach for the solution of these equations. With this approach, which corresponds to the nature of the PNS equations steady supersonic viscous flows are calculated with CPU times and computer memo-

ries much less than those used by a Navier-Stokes code. Since PNS equations are derived from Navier-Stokes equations, they include all terms of Euler equations and therefore are valid in both inviscid and viscous regions.

The main drawback of PNS equations, however, is that they can not be used for analysis of flows with upstream effects or with embedded separated regions. One approach for the analysis of such flows is to use a NS code for separated regions and a PNS code for the rest of the domain. Be-